

**EXTRACTION AND ANALYSIS OF PRESOLAR GRAINS FROM THE LAP 031117 CO 3.0 CHONDRITE.** T. J. Zega<sup>1</sup>, P. Haenecour<sup>2,3</sup>, C. Floss<sup>2,4</sup>, and R. M. Stroud<sup>5</sup>. <sup>1</sup>Lunar and Planetary Laboratory, University of Arizona, Tucson, AZ 85721, USA. <sup>2</sup>Laboratory for Space Sciences, <sup>3</sup>Dept. of Earth and Planetary Sciences, <sup>4</sup>Physics Department, Washington University, St. Louis, MO 63130, USA. <sup>5</sup>Code 6366, Naval Research Laboratory, 4555 Overlook Avenue, Washington DC 20375. (tzega@lpl.arizona.edu).

**Introduction:** Refractory dust grains formed during the dying stages of ancient stars were injected into the local part of our galaxy where our solar system formed over 4.5 billion years ago. Such presolar circumstellar materials were incorporated into primitive meteorites, the physical relics leftover from our solar system's birth. Locked up within their crystal chemistry and structure is a snapshot of the state of the star at the very moment that the circumstellar grain condensed. Probing these materials can provide ground-truth information on nucleosynthetic processes that occurred in their parent stars, the thermodynamics that took place in the circumstellar envelopes from which they condensed, transport and irradiation processes within the interstellar medium, and secondary processes that could have affected them during solar system evolution [1,2].

Historically, acid-dissolution techniques have provided abundant presolar grains (e.g., graphites, SiC, and oxides) for detailed analysis. However, such an approach destroys the petrographic context of the grains and thus potential evidence of secondary processing, e.g., parent-body alteration or radiation processing in the interstellar medium. Here we expand on our previous efforts to investigate presolar grains *in situ*, and report results on three grains from the LAP 031117 CO3.0 chondrite.

**Experimental:** Isotopic mapping via secondary ion mass spectrometry (SIMS) revealed 112 oxygen-anomalous presolar grains in LAP 031117 [3]. We chose three of these grains for microstructural analysis: LAP-81 from the matrix and LAP-103 and LAP-104 from a fine-grained chondrule rim. The grains and surrounding matrix material were extracted and thinned to electron transparency with an FEI Nova 200 focused-ion-beam scanning-electron microscope (FIB-SEM) at Arizona State University using previously described methods [4]. Fiducial Pt markers were placed on top of the grains prior to cross sectioning to ensure accurate locations of the FIB transects. Grain microstructure and chemistry was investigated at the Naval Research Lab using a 200 keV JEOL 2200FS transmission electron microscope (TEM) equipped with an ultrathin window energy-dispersive Si(Li) X-ray spectrometer (EDS) and scanning-based TEM (STEM) bright- and high-angle annular dark-field (HAADF) detectors.

**Results:** The three grains selected belong to the Group-1 field for presolar oxides [5], with enrichments in  $^{17}\text{O}$  and close-to-solar  $^{18}\text{O}/^{16}\text{O}$  ratios (LAP-81:

$$^{17}\text{O}/^{16}\text{O} = 12.2 \pm 0.3 \times 10^{-4} \text{ and } ^{18}\text{O}/^{16}\text{O} = 1.52 \pm 0.05 \times 10^{-3}; \text{ LAP-103: } ^{17}\text{O}/^{16}\text{O} = 35.5 \pm 0.6 \times 10^{-4} \text{ and } ^{18}\text{O}/^{16}\text{O} = 2.05 \pm 0.04 \times 10^{-3}; \text{ and LAP-104: } ^{17}\text{O}/^{16}\text{O} = 21.0 \pm 0.6 \times 10^{-4} \text{ and } ^{18}\text{O}/^{16}\text{O} = 2.16 \pm 0.05 \times 10^{-3}$$

Figure 1 (top) shows the FIB section through LAP-81. Pt fiducial markers, deposited prior to cross sectioning, indicate the O-anomalous region. Bright-field (BF) TEM imaging shows that this area measures  $\approx 1 \mu\text{m}$  wide and contains a grain at the center measuring  $\approx 256 \text{ nm}$  across. Selected-area electron-diffraction (SAED) patterns reveal that the grain is crystalline but with slightly different orientations on the left ( $\approx 130 \text{ nm}$ ) and right ( $\approx 126 \text{ nm}$ ) sides. The SAED patterns index to olivine. High-resolution TEM (HRTEM) confirms the slight orientation change. EDS measurements show that the grain contains abundant Fe, Mg, Si, O, and minor Ca. Quantification of EDS spectra suggests non-stoichiometry for the left side of the grain, whereas the right side is stoichiometric Ca-bearing olivine.

Figure 1 (bottom) shows the FIB section through LAP-103 and -104. The area corresponding to LAP-103 contains a grain measuring  $\approx 782 \text{ nm}$  wide. EDS shows that the grain is composed of Fe and O. SAED patterns reveal that the grain is crystalline and index to magnetite. Quantification of EDS spectra conforms to  $\text{Fe}_3\text{O}_4$ . In comparison, BF-TEM imaging of the area corresponding to LAP-104 reveals a fine-grained ( $\approx 10$  to  $70 \text{ nm}$ ) mixture of material. EDS shows that the area contains Fe-Mg-Al-Ca silicate bearing materials and SAED patterns show that it is polycrystalline, with multiple *d*-spacings that overlap with olivine and pyroxene.

**Discussion:** The isotopic compositions of presolar oxide grains reflect the formation and evolutionary histories of the progenitor stars from which they condensed. The O-isotopic compositions of the three grains studied here indicate that they are Group-1 grains, which formed within the circumstellar envelopes of low- to intermediate-mass RGB/AGB stars of close-to-solar metallicity.

The TEM data reveal discrete circumstellar grains for LAP-81 and LAP-103. In comparison, the TEM data on LAP-104 show a polycrystalline assemblage of fine-grained material, making pinpointing a single-phase carrier of the O anomaly, and hence, an individual circumstellar grain, difficult. Rather, the data point toward the entire polycrystalline assemblage beneath the Pt marker as the 'grain'. We note that fine-grained

polycrystalline and amorphous aggregates of presolar silicates have been previously identified in situ within, e.g., O-anomalous regions of the Acfer 094, MET 00426, and ALHA 77307 chondrites [6-8]. Non-equilibrium condensation, multistep condensation, post-condensation annealing, and irradiation in the ISM have been proposed to explain such polycrystallinity and chemical heterogeneity. We have not observed amorphous grains within the area of LAP-104, but the chemical heterogeneity may point to non-equilibrium or multistep condensation.

The TEM data show that LAP-81 is a Ca-bearing olivine. Equilibrium thermodynamic calculations predict that olivine will condense from a gas of solar composition over a range of pressure and temperature, but such calculations suggest that the olivine is mostly forsteritic in composition [see 9, and plate 7]. Calculations by [10] showed that the FeO content of silicates can be increased to  $\text{FeO}/(\text{FeO} + \text{MgO})$  molar ratios of 0.1 to 0.4 if the condensing system is enriched in chondritic vapor. The EDS spectra acquired for LAP-81 give  $\text{FeO}/(\text{FeO} + \text{MgO})$  ratios of approximately 0.5, slightly above the maximum estimated by [10] for dust-enriched systems, which argues against equilibrium condensation for this grain. The FeO contents of silicates can be enriched during secondary alteration on the parent body [e.g., 11]. Parent-body processing has been inferred previously for Fe enrichments in presolar silicate grains in the matrix of the Adelaide C2 ungrouped chondrite [12], but we do not observe evidence for such processing from the FIB sections of LAP 031117. The high Fe contents, as well as the non-stoichiometric composition of the left domain of LAP-81, thus possibly point to non-equilibrium condensation. We note that high Fe contents are common in presolar silicate grains and have led to similar conclusions [13,14].

The TEM data identify LAP-103 as a grain of magnetite. To our knowledge, this is the first definitive microstructural identification of presolar magnetite. We note that [15] identified a magnetite subgrain ( $\approx 30$  nm) in a ultramicrotome section of a presolar graphite, but its small size precluded isotopic analysis and thus verification of its presolar origin. The formation of magnetite in the solar system is somewhat controversial, and multiple pathways, including secondary alteration, have been proposed [e.g., 16-18]. As noted above, we find no evidence in these FIB sections for aqueous-phase reactions on the LAP 031117 parent body that would otherwise explain the formation of the observed magnetite. An alternative pathway for magnetite formation is the oxidation of preexisting Fe metal grains [19]. In this pathway, magnetite is formed through reaction of previously condensed Fe metal with O in the gas. We hypothesize that such a pathway could be responsible for the formation of LAP-103.

**References:** [1] Zinner E.K. (2004) *Treatise on Geochemistry*, Vol. 1, 17-39. [2] Bernatowicz T.J. et al., (2006) *MESS II*, 109-126. [3] Haenecour P. et al. (2013) *LPSC XLIII*, #1107. [4] Zega T.J. et al. (2007) *MaPS* 42, 1373-1386. [5] Nittler L.R. et al. (2008) *Ap.J.* 682, 1450-1478. [6] Vollmer C. et al. (2009) *Ap.J.* 700, 774-782. [7] Stroud R.M. et al. (2009) *LPSC XL*, #1063. [8] Nguyen A.N. et al. (2010) *Ap.J.* 719, 166-189. [9] Ebel D.S. (2006) Meteorites and the Early Solar System II 253-277. [10] Ebel D.S. and Grossman L. (2000) *GCA* 64, 339-366. [11] Brearley A.J. (2003) *Treatise on Geochemistry*, Vol. 1: Meteorites, Comets, and Planets (A.M. Davis, ed) 247-268. [12] Floss C. and Stadermann F. (2012) *MaPS* 47, 992-1009. [13] Nguyen et al. (2007) *Ap. J.* 656, 1223-1240. [14] Bose M. et al. (2010) *ApJ* 714, 1624-1636. [15] Croat et al. (2008) *MaPS* 43, 1497-1515. [16] Kerridge J.F. (1970) *EPSL* 9, 299-306. [17] Nagahara H. (1984) *GCA* 48, 2581-2595. [18] Kerridge J.F. et al. (1979) *Science* 205, 395-397. [19] Hong Y. and Fegley B, Jr. (1998) *MaPS* 33, 1101-1112.

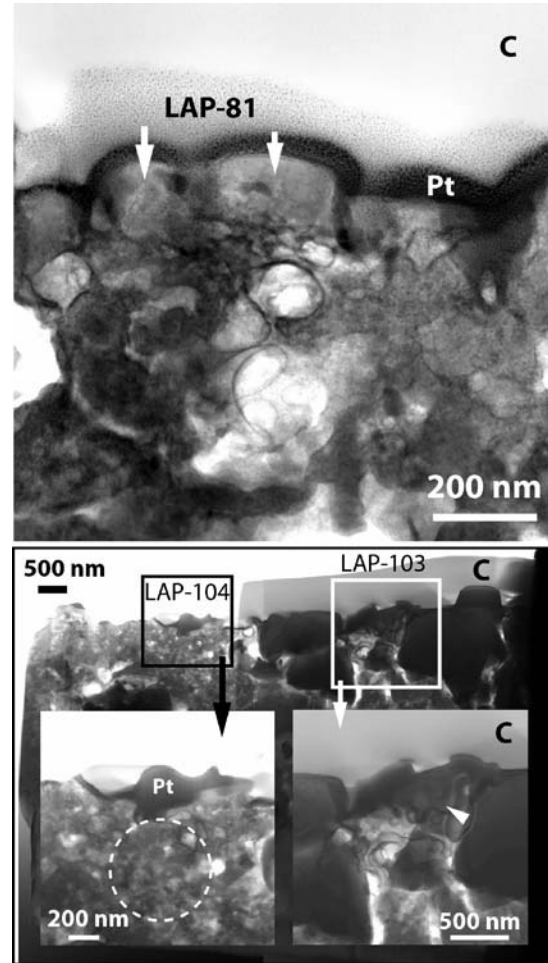


**Fig. 1.** TEM data on LAP 031117. **(top)** BF-STEM image of LAP-81. **(bottom)** BF-STEM image of LAP-103 and -104. Higher-magnification images inset. LAP-103 indicated by arrow and dashed circle, respectively. C strap and Pt fiducial markers indicated.